ARTICLE

Coherent Control of Multiple 2nd-Order Quantum Pathways†

Fang Gao[a], Yao-xiong Wang[a,b], De-wen Cao[a,b], Feng Shuang[a,b*]

a. Institute of Intelligent Machines, Chinese Academy of Sciences, Hefei 230031, China
b. Department of Automation, University of Science and Technology of China, Hefei 230027, China

(Dated: Received on June 15, 2015; Accepted on July 13, 2015)

The manipulation of two 2nd-order quantum pathways has been successfully demonstrated experimentally in atomic Rubidium. This work would explore the coherent control of pathways in the quantum system with N intermediate states connecting the initial and target states. A $4N$-block scheme is proposed to control the N 2nd-order pathways which are driven by a weak broadband pulse. The model with N=3 is given as an example to demonstrate our strategy. In this scheme, boundaries of the spectral blocks are functions of the resonant frequencies, and the resonant and non-resonant contributions interfere mutually to achieve the quantum pathway control effectively. The simple strategy may provide a practical choice for pathway manipulation experiments since there are only $2N$ phase variables to adjust.

Key words: Coherent control, Multiple 2nd-order, Quantum pathway

I. INTRODUCTION

Due to its scientific importance and potential applications, quantum dynamics control has been an attractive field [1–5]. In many laser experiments, coherent control of an observable is often achieved by adjusting the interference among different quantum pathways [6, 7]. Thus, it is important to investigate pathway manipulation in quantum systems. Recently, Rey-de-Castro *et al.* have successfully controlled the ratio of two 2nd-order quantum pathways in Rubidium [8]. Their experiments show that the quantum pathway dynamics can be steered towards the desired direction by phase shaping of broadband femtosecond pulses. We have also investigated the cooperation and competition between pathways in the the optimal control of Rubidium [9].

Silberberg *et al.* have proposed that a resonant two-photon absorption (TPA) rate can be enhanced via constructive interference between resonant and non-resonant contributions [10]. In their work, a three-level ladder configuration is employed with only one 2nd-order pathway involved. Based on Silberberg's work, Lee *et al.* have proposed an eight-block scheme to maximize the fluorescence signal from the target state for a four-level diamond configuration system with two 2nd-order pathways involved [11].

In this work, we further study the manipulation of multiple 2nd-order pathways. Compared with the transform limited pulses (TLPs), the $4N$ block scheme with only $2N$ phase variables to adjust can achieve much better effects, as illustrated by an example with three intermediate states.

II. THEORETICAL MODEL

We consider a quantum system with N intermediate states connecting the initial stand target states. The Hamiltonian is the form of $H=H_0-\mu E(t)$, where H_0 is the unperturbed Hamiltoni with eigenstates $|l_p\rangle$ (p=0, 1, ..., N, $N+1$), μ is the dipole moment operator, and $E(t)$ is the control field. In the basis $\{|l_p\rangle\}$, the matrices H_0 and μ are given by

$$H_0 = \begin{bmatrix} 0 & 0 & 0 & \cdots & 0 & 0 \\ 0 & \omega_1 & 0 & \cdots & 0 & 0 \\ 0 & 0 & \omega_2 & \cdots & 0 & 0 \\ \vdots & \vdots & \vdots & \cdots & \vdots & \vdots \\ 0 & 0 & 0 & \cdots & \omega_N & 0 \\ 0 & 0 & 0 & \cdots & 0 & \omega_{N+1} \end{bmatrix} \tag{1}$$

$$\mu = \begin{bmatrix} 0 & \mu_1 & \mu_2 & \cdots & \mu_N & 0 \\ \mu_1 & 0 & 0 & \cdots & 0 & \mu'_1 \\ \mu_2 & 0 & 0 & \cdots & 0 & \mu'_2 \\ \vdots & \vdots & \vdots & \cdots & \vdots & \vdots \\ \mu_N & 0 & 0 & \cdots & 0 & \mu'_N \\ 0 & \mu'_1 & \mu'_2 & \cdots & \mu'_N & 0 \end{bmatrix} \tag{2}$$

where atomic units are adopted with $\hbar$=1. The initial state is $|l_0\rangle$ with zero energy, and the target state is $|l_{N+1}\rangle$ with energy ω_{N+1}. There are N intermediate states $|l_p\rangle$ (p=1, ..., N). An example system with N=3 is shown in Fig.1(a).

The dynamics in the interaction representation are

†Dedicated to Professor Qing-shi Zhu on the occasion of his 70th birthday.

*Author to whom correspondence should be addressed. E-mail: shuangfeng@ustc.edu.cn

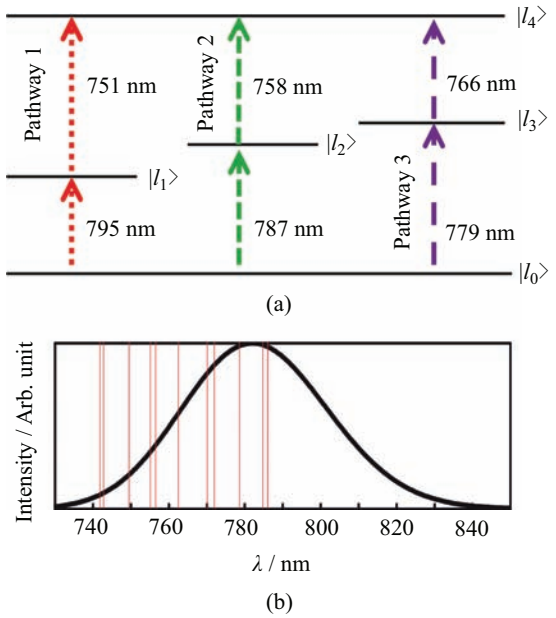

FIG. 1 (a) Energy level structure of the example system. The three 2nd-order pathways are $|l_0\rangle\rightarrow|l_1\rangle\rightarrow|l_4\rangle$, $|l_0\rangle\rightarrow|l_2\rangle\rightarrow|l_4\rangle$, and $|l_0\rangle\rightarrow|l_3\rangle\rightarrow|l_4\rangle$. (b) Spectrum of the laser pulse ($E_0(\omega)$ in Eq.(8)) employed in our theoretical studies. The spectrum is divided into 12 blocks in our strategy, and the vertical lines indicate the spectral boundaries. Each block has a constant phase.

governed by

$$i\frac{\mathrm{d}U_I(t)}{\mathrm{d}t} = V_I(t)U_I(t) \tag{3}$$

where $U_I(t)$ is the evolution operator and

$$V_I(t) = -\exp(iH_0t)\mu E(t)\exp(-iH_0t) \tag{4}$$

In the perturbation regime, N 2nd-order pathways, $|l_0\rangle\rightarrow|l_p\rangle\rightarrow|l_{N+1}\rangle$ (p=1, $\cdots$, N), dominate the excitation from the initial state $|l_0\rangle$ to the target state $|l_{N+1}\rangle$. The corresponding amplitudes are given by the following N 2nd-order Dyson expansion terms of $U_I(t)$,

$$U_p(T) = -\mu_p\mu'_p\int_{-\infty}^{T}\exp[i\,(\omega_{N+1}-\omega_p)\,t_2]E(t_2)\cdot$$
$$\int_{-\infty}^{t_2}\exp[i\omega_p t_1]E(t_1)\mathrm{d}t_1\mathrm{d}t_2,$$
$$p = 1,\ 2,\ \cdots,\ N \tag{5}$$

The final amplitude of each pathway after the pulse is over ($T\rightarrow\infty$) can be written in the frequency domain as combination of resonant part U_p^r and non-resonant part U_p^{nr} [10]

$$U_p(T\rightarrow\infty) = U_p^r + U_p^{nr}$$
$$= \mu_p\mu'_p\Big[-\pi E(\omega_p)E(\omega_{N+1}-\omega_p) +$$
$$i\wp\int_{-\infty}^{\infty}\frac{E(\omega)E(\omega_{N+1}-\omega)}{\omega_p-\omega}\mathrm{d}\omega\Big] \tag{6}$$

here $\wp$ is the principal value of Cauchy. Then the total transition probability from the initial state $|l_0\rangle$ to the target state $|l_{N+1}\rangle$ after the pulse being off is

$$P_f = |\langle l_{N+1}|U_I(T\rightarrow\infty,0)|l_0\rangle|^2$$
$$\approx \left|\sum_{p=1}^{N}U_p(T\rightarrow\infty)\right|^2_{T\rightarrow\infty} \tag{7}$$

III. PATHWAY MANIPULATION STRATEGY

To mimic the experimental conditions, a laser field with a Gaussian envelope is employed in our studies:

$$E(\omega) = E_0(\omega)\exp i\varphi(\omega) \tag{8}$$

$$E_0(\omega) = B\exp\left[\frac{-(\omega-\omega_0)^2}{\triangle^2}\right]\exp[i\varphi(\omega)] \tag{9}$$

here the parameter B is taken to be 0.0006 a.u., small enough to make sure that the light-atom interaction is perturbative. In our strategy, only the phase $\varphi(\omega)$ is adjusted to control the quantum pathways.

As shown in Eq.(6), each pathway amplitude can be divided into the resonant and non-resonant parts, and thus it can be modulated by changing the interference of these terms. Our pathway manipulation strategy is based on this idea, and one five-level quantum system will be used as an example in the following for demonstration.

The example system is shown in Fig.1(a) with the parameters in Eq.(1) and Eq.(2) being μ_1=0.95, μ_2=1.01, μ_3=1.1, μ'_1=1.22, μ'_2=1.15, μ'_3=1.06, ω_1=0.0573 ($\sim$795 nm), ω_2=0.0579 ($\sim$787 nm), ω_3=0.0585 ($\sim$779 nm), and ω_4=0.118 ($\sim$386 nm). The spectrum of the laser pulse employed in our studies is shown in Fig.1(b), with the central frequency ω_0 and full width at half maximum (FWHM) of the pulse being 0.0583 ($\sim$782 nm) and 0.00335 ($\sim$45 nm), respectively.

Three 2nd-order pathways, namely $|l_0\rangle\rightarrow|l_1\rangle\rightarrow|l_4\rangle$, $|l_0\rangle\rightarrow|l_2\rangle\rightarrow|l_4\rangle$, and $|l_0\rangle\rightarrow|l_3\rangle\rightarrow|l_4\rangle$, dominate the population transfer from the initial state $|l_0\rangle$ to the target state $|l_4\rangle$. The non-resonant term of the pth (p=1, 2, 3) pathway is

$$U_p^{nr} = i\mu_p\mu'_p\wp\int_{-\infty}^{\infty}\Big\{\frac{E_0(\omega)E_0(\omega_4-\omega)}{\omega_p-\omega}\cdot$$
$$\exp[i\varphi(\omega)]\exp[i\varphi(\omega_4-\omega)]\Big\}\mathrm{d}\omega \tag{10}$$

Then the total non-resonant contribution is

DOI:10.1063/1674-0068/28/cjcp1506124

$$U^{nr} = i\wp \int_{-\infty}^{\infty} \{f(\omega)E_0(\omega)E_0(\omega_4-\omega) \exp[i\varphi(\omega)]\exp[i\varphi(\omega_4-\omega)]\}\mathrm{d}\omega \quad (11)$$

$$f(\omega) = \sum_{p=1}^{3} \frac{\mu_p\mu'_p}{\omega_p-\omega} = -(\mu_1\mu'_1+\mu_2\mu'_2+\mu_3\mu'_3)\cdot \frac{(\omega-\omega_{c1})(\omega-\omega_{c2})}{(\omega-\omega_1)(\omega-\omega_2)(\omega-\omega_3)} \quad (12)$$

where ω_{c1} and ω_{c2} are the two zero points of $f(\omega)$. Thus $f(\omega)$ changes its plus-minus sign around five critical frequencies ω_1, ω_{c1}, ω_2, ω_{c2} and ω_3. The population transfer is a two-photon process with the sum frequency of the two photons being ω_4. Eq.(6) indicates that each pathway amplitude depends on the phase function $\varphi(\omega)+\varphi(\omega_4-\omega)$, which is symmetrically added around $\omega_4/2$. Hence, we should add five more critical frequencies which are symmetric about $\omega_4/2$ and get 11 critical frequencies totally, as shown in Fig.2. A simple strategy to coherently control the transition process is to divide the spectrum into 12 blocks by these 11 critical frequencies, with the spectral blocks labeled as B_1, B_2, $\cdots$, B_{12}, and each having a constant phase,

$$\varphi(\omega) = \overline{\varphi}_j, \quad \omega \in \text{block}\, B_j \quad (13)$$

Then the individual and sum non-resonant contributions will only depend on the combinational phase $\overline{\varphi}_j + \overline{\varphi}_{13-j}$:

$$U_p^{nr} = \sum_{j=1}^{6} U_{p,B_j}^{nr} \exp[i(\bar{\varphi}_j + \bar{\varphi}_{13-j})] \quad (14)$$

$$U^{nr} = \sum_{j=1}^{6} U_{B_j}^{nr} \exp[i(\bar{\varphi}_j + \bar{\varphi}_{13-j})] \quad (15)$$

with the term U_{p,B_j}^{nr} representing the pth pathway contribution from blocks B_j and B_{13-j},

$$U_{p,B_j}^{nr} = i\mu_p\mu'_p \int_{B_j \bigcup B_{13-j}} \frac{E_0(\omega)E_0(\omega_4-\omega)}{\omega_p-\omega}\mathrm{d}\omega \quad (16)$$

$$U_{B_j}^{nr} = i\sum_{p=1}^{3} U_{p,B_j}^{nr} \quad (17)$$

Without loss of generality, we could set the phases of the last six blocks to zero, then the non-resonant terms depend on only phases of the first six blocks:

$$U_p^{nr} = \sum_{j=1}^{6} U_{p,B_j}^{nr} \exp(i\bar{\varphi}_j) \quad (18)$$

$$U^{nr} = \sum_{j=1}^{6} U_{B_j}^{nr} \exp(i\bar{\varphi}_j) \quad (19)$$

Therefore, the pathway amplitudes can be coherently controlled by changing the six block phases. Our pathway manipulation strategy is tested for six cases with different objective functions with the results shown in Table I.

From the top panel of Fig.2, the conditions to maximize $|U_1|$, $|U_2|$, $|U_3|$, and $\left|\sum_p U_p\right|$ can be easily extracted: φ_1=$\pi/2$ and φ_2=φ_3=φ_4=φ_5=φ_6=$-\pi/2$ for $|U_1|$ maximization; φ_1=φ_2=φ_3=$\pi/2$ and φ_4=φ_5=φ_6=$-\pi/2$ for $|U_2|$ maximization; φ_1=φ_2=φ_3=φ_4=φ_5=$\pi/2$ and φ_6=$-\pi/2$ for $|U_3|$ maximization; φ_1=φ_3=φ_5=$\pi/2$ and φ_2=φ_4=φ_6=$-\pi/2$ for $\left|\sum_p U_p\right|$ maximization. In consistent with the above analysis, Table I shows nearly the same simulation results for the first four cases, in which a finite difference-based gradient method is employed in the optimization. For the last three cases, the objective functions are chosen to be the pathway ratios to redirect the dynamics to desired pathways. The simulations turn out that we could keep the amplitude of the desired pathway the same order of magnitude as its maximal value in the first three cases, while suppressing the amplitudes of the other two pathways by several orders of magnitude. For example, in last column, amplitude of pathway 3 is 3.8636×10^{-5}, which is just a little smaller than 5.1419×10^{-5}, the best amplitude we could get, while the amplitude of pathways 1 and 2 are suppressed to less than 4×10^{-11}. For TLPs, the pathway amplitudes are 5.4079×10^{-7} ($|U_1|$), 7.0474×10^{-7} ($|U_2|$), 8.2938×10^{-7} ($|U_3|$) and 1.9726×10^{-6} $\left(\left|\sum_p U_p\right|\right)$. Compared with TLPs, the objective functions can be improved by several orders of magnitude, which validates the success of this simple pathway manipulation strategy.

Above strategy can be extended to quantum systems with N intermediate states ($|l_p\rangle$, p=1, …, N) connecting the initial ($|l_0\rangle$) and target ($|l_{N+1}\rangle$) states. The procedures can be summarized as the following three steps: (i) The phases at the resonant frequencies ω_p and $\omega_{N+1}-\omega_p$ are set to be zero. (ii) The whole spectrum is divided into $4N$ blocks, with the boundaries being ω_p, $\omega_{N+1}-\omega_p$, $\omega_N/2$, ω_c, and $\omega_{N+1}-\omega_c$, where ω_c satisfies,

$$\sum_{p=1}^{N} \frac{\mu_p\mu'_p}{\omega_p-\omega_c} = 0 \quad (20)$$

(iii) Only those of the first spectral $2N$ blocks are optimized, while the phases of the last $2N$ spectral blocks are fixed to zero. The strategy can effectively manipulate quantum control pathways via changing only $2N$ phase variables. It is simple and thus easy to implement in the experiments.

DOI:10.1063/1674-0068/28/cjcp1506124

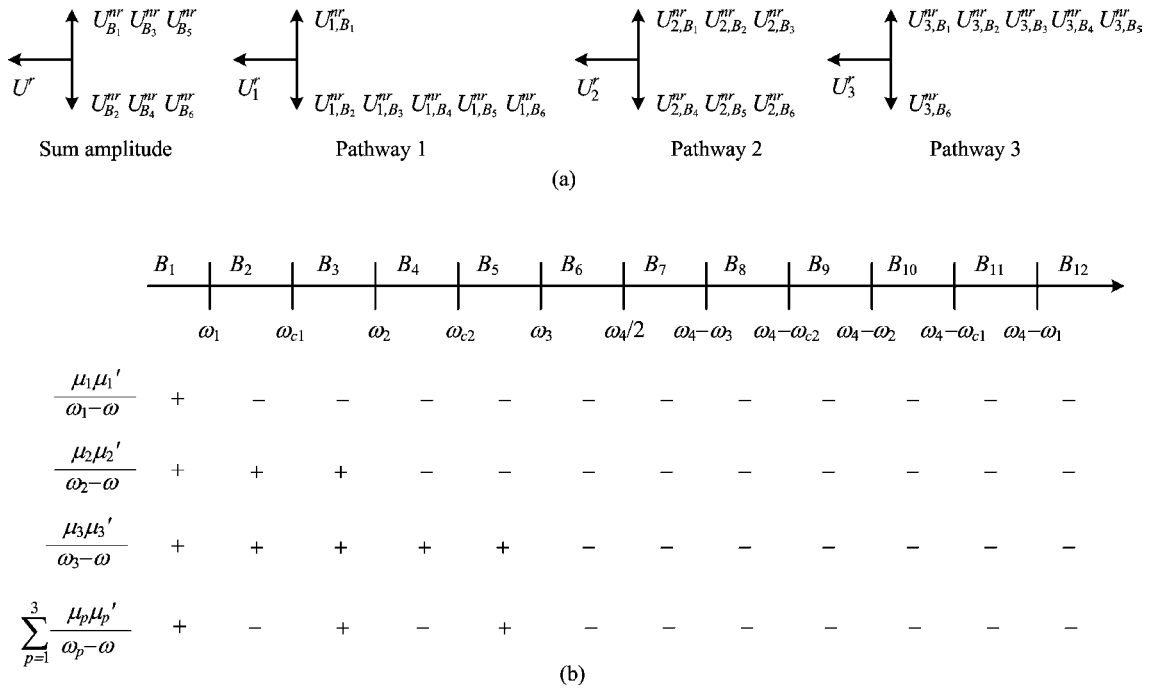

FIG. 2 (a) For transform limited pulses with zero phases in all blocks, the resonant and non-resonant terms of the sum and individual pathway amplitudes are shown in the complex plane. (b) In our strategy, the whole spectrum is divided into 12 blocks, with the boundaries ω_1, ω_{c1}, ω_2, ω_{c2}, ω_3, $\omega_4/2$, $\omega_4-\omega_3$, $\omega_4-\omega_{c2}$, $\omega_4-\omega_2$, $\omega_4-\omega_{c1}$ and $\omega_4-\omega_1$. The non-resonant terms are decomposed into 6 parts (B_1, B_2, ..., B_6 in (a)), with each part B_j corresponding to contributions from two paired spectral blocks B_j and B_{13-j}, as shown in Eq.(16). The signs of the integral kernels of different non-resonant terms are indicated for each spectral block.

TABLE I The optimization results under different objective functions. Here cons. denotes a constant small enough, which is taken to be 1.0×10^{-8} in our simulations.

	$\lvert U_1\rvert$	$\lvert U_2\rvert$	$\lvert U_3\rvert$	$\lvert U_1+U_2+U_3\rvert$	$\frac{\lvert U_1\rvert}{\lvert U_2\rvert+\lvert U_3\rvert+\text{cons.}}$	$\frac{\lvert U_2\rvert}{\lvert U_1\rvert+\lvert U_3\rvert+\text{cons.}}$	$\frac{\lvert U_3\rvert}{\lvert U_1\rvert+\lvert U_2\rvert+\text{cons.}}$
	(Case I)	(Case II)	(Case III)	(Case IV)	(Case V)	(Case VI)	(Case VII)
φ_1	0.5000π	0.5000π	0.5000π	0.5000π	0.4868π	-0.0119π	0.1644π
φ_2	-0.5000π	0.5000π	0.5000π	-0.5000π	-0.4318π	-0.0140π	0.1777π
φ_3	-0.5000π	0.5000π	0.5000π	0.5000π	0.4151π	0.6296π	-0.0486π
φ_4	-0.5000π	-0.5000π	0.5000π	-0.5000π	0.4221π	-0.2908π	-0.0390π
φ_5	-0.5000π	-0.5000π	0.5000π	0.5000π	0.1727π	0.4782π	0.4797π
φ_6	-0.5000π	-0.5000π	-0.5000π	-0.5000π	0.1834π	0.4768π	-0.9777π
$\lvert U_1\rvert$	1.4323×10^{-5}	3.9295×10^{-7}	3.0251×10^{-8}	1.3882×10^{-5}	1.3284×10^{-5}	4.6584×10^{-11}	3.8258×10^{-11}
$\lvert U_2\rvert$	1.0438×10^{-6}	3.2291×10^{-5}	4.7377×10^{-7}	3.2106×10^{-5}	1.0725×10^{-10}	3.1308×10^{-5}	1.1819×10^{-11}
$\lvert U_3\rvert$	1.1013×10^{-6}	$1.1852\text{e}\times10^{-6}$	5.1419×10^{-5}	5.0921×10^{-5}	3.4529×10^{-11}	9.3307×10^{-11}	3.8636×10^{-5}
$\lvert U_1+U_2+U_3\rvert$	1.6469×10^{-5}	3.3869×10^{-5}	5.1923×10^{-5}	9.6909×10^{-5}	1.3284×10^{-5}	3.1308×10^{-5}	3.8636×10^{-5}

IV. CONCLUSION

Coherent control of pathway is investigated in the perturbation regime for quantum systems with N intermediate states connecting the initial and target states, and a simple but effective strategy is proposed. In the strategy, the overall spectrum is divided into $4N$ blocks, and only the phases of the first $2N$ blocks are optimized. An example with N=3 is given for demonstration. The strategy provides a practical choice for pathway manipulation in the optimal control experiments. It has to be noted that there are at most $N-1$ critical frequencies that fulfill Eq.(20) and lead to $4N$ spectral blocks. If Eq.(20) has less than $N-1$ real roots, the number of spectral blocks could be less than $4N$, and further discussion is necessary.

DOI:10.1063/1674-0068/28/cjcp1506124

V. ACKNOWLEDGMENTS

This work was supported by the National Natural Science Foundation of China (No.61203061, No.61403362, No.61374091, and No.61473199).

[1] J. M. Geremia, J. K. Stockton, and H. Mabuchi, Science **304**, 270 (2004).
[2] H. M. Wiseman and A. C. Doherty, Phys. Rev. Lett. **94**, 070405 (2005).
[3] H. Rabitz, R. de Vivie-Riedle, M. Motzkus, and K. Kompa, Science **288**, 824 (2000).
[4] N. Yamamoto, H. I. Nurdin, M. R. James, and I. R. Petersen, Phys. Rev. A **78**, 042339 (2008).
[5] J. Zhang, R. B. Wu, C. W. Li, and T. J. Tarn, IEEE T. Automat. Contr. **55**, 619 (2010).
[6] D. Meshulach and Y. Silberberg, Nature **396**, 239 (1998).
[7] R. Netz, A. Nazarkin, and R. Sauerbrey, Phys. Rev. Lett. **90**, 063001 (2003).
[8] R. Rey-de-Castro, Z. Leghtas, and H. Rabitz, Phys. Rev. Lett. **110**, 223601 (2013).
[9] F. Gao, R. Rey-de-Castro, A. M. Donovan, J. Xu, Y. Wang, H. Rabitz, and F. Shuang, Phys. Rev. A **89**, 023416 (2014)
[10] N. Dudovich, B. Dayan, S. M. G. Faeder, and Y. Silberberg, Phys. Rev. Lett. **86**, 47 (2001).
[11] H. Lee, H. Kim, J. Lim, and J. Ahn, Phys. Rev. A **88**, 053427 (2013).

DOI:10.1063/1674-0068/28/cjcp1506124